Separation Science and Technology
Publication details, including instructions for authors and subscription information:
http://www.informaworld.com/smpp/title~content=t713708471

ADSORPTION OF RADIOACTIVE METALS BY STRONGLY MAGNETIC IRON SULFIDE NANOPARTICLES PRODUCED BY SULFATE-REDUCING BACTERIA

J. H. P. Watson[a]; I. W. Croudace[b]; P. E. Warwick[b]; P. A. B. James[c]; J. M. Charnock[d]; D. C. Ellwood[e]
[a] Department of Physics and Astronomy, Daresbury Warrington, Cheshire, UK [b] School of Ocean and Earth Science, SOC, Cheshire, UK [c] Department of Civil and Environmental Engineering, Daresbury Warrington, Cheshire, UK [d] Daresbury Laboratory, Cheshire, UK [e] University of Southampton, Southhampton, UK

Online publication date: 30 November 2001

To cite this Article Watson, J. H. P. , Croudace, I. W. , Warwick, P. E. , James, P. A. B. , Charnock, J. M. and Ellwood, D. C.(2001) 'ADSORPTION OF RADIOACTIVE METALS BY STRONGLY MAGNETIC IRON SULFIDE NANOPARTICLES PRODUCED BY SULFATE-REDUCING BACTERIA', Separation Science and Technology, 36: 12, 2571 — 2607
To link to this Article: DOI: 10.1081/SS-100107214
URL: http://dx.doi.org/10.1081/SS-100107214

SEPARATION SCIENCE AND TECHNOLOGY, 36(12), 2571–2607 (2001)

ADSORPTION OF RADIOACTIVE METALS BY STRONGLY MAGNETIC IRON SULFIDE NANOPARTICLES PRODUCED BY SULFATE-REDUCING BACTERIA

J. H. P. Watson,[1,*] I. W. Croudace,[2] P. E. Warwick,[2] P. A. B. James,[3] J. M. Charnock,[4] and D. C. Ellwood[5]

[1]Department of Physics and Astronomy, [2]School of Ocean and Earth Science, SOC, [3]Department of Civil and Environmental Engineering, and [4]Daresbury Laboratory, Daresbury Warrington, Cheshire WA4 4AD, UK
[5]Visiting Professor, University of Southampton, Southhampton, UK

ABSTRACT

The adsorption of a number of radioactive ions from solution by a strongly magnetic iron sulfide material was studied. The material was produced by sulfate-reducing bacteria in a novel bioreactor. The uptake was rapid and loading on the adsorbent was high due to the high surface area of the adsorbent and because many of the ions were chemisorbed. The structural properties were examined with high-resolution imaging and electron diffraction by transmission electron microscopy. The adsorbent surface area was determined to be 400–500m^2/g by adsorption of heavy metals, the magnetic properties, neutron scattering, and transmission electron microscopy. The adsorption of a number of radionuclides was

*Corresponding author. Fax: 44-238-0593910; E-mail: jhpw@soton.ac.uk

examined at considerably lower concentration than in previous work with these adsorbent materials. A number of ions studied are of interest to the nuclear industry, particularly the pertechnetate ion (TcO_4^-). ^{99}Tc is a radionuclide thought to determine the long-term environmental impact of the nuclear fuel cycle because of its long half-life and because it occurs normally in the form of the highly soluble pertechnetate ion, which can enter the food chain. This bacteria-generated iron sulfide may provide a suitable matrix for the long-term safe storage of the pertechnetate ion. Also, because of the prevalence of the anaerobic sulfate-reducing bacteria worldwide and, in particular, in sediments, the release of radioactive heavy metals or toxic heavy metals into the environment could be engineered so that they are immobilized by sulfate-reducing bacteria or the adsorbents that they produce and removed from the food chain.

INTRODUCTION

This paper describes the adsorption of a number of radionuclides, some of which are of interest to the nuclear industry, by a strongly magnetic iron sulfide produced through a new method involving sulfate-reducing bacteria (SRB) (1). This work follows from previous adsorption studies of metal ions on a weakly magnetic ion sulfide produced by sulfate-reducing bacteria (2).

The use of radioactive ions in this work has two advantages. First, the adsorption processes can be evaluated at much lower metal ion concentrations than is possible with atomic absorption spectroscopy used in the previous work. Second, it provides an opportunity to study the adsorption of metal ions that may be of practical value to the nuclear industry. Of particular interest is the adsorption of technetium (in the form of the pertechnetate ion TcO_4^-) from solution, which has proved a problem for the nuclear industry because it is not effectively removed by the processes presently used for effluent treatment. ^{99}Tc may be the critical radionuclide in determining the long-term environmental impact of the nuclear fuel cycle (3). Because ^{99}Tc is a long-lived pure β emitter with a half-life of 2.13×10^5 years, it usually occurs in the form of the pertechnetate ion (TcO_4^-), which is highly soluble and environmentally mobile (4). Furthermore, TcO_4^- can be readily taken up by plants (5) and enter the food chain; Cataldo et al. (6) suggested that in many cases, Tc enters the food chain as a sulfate analogue. The level of ^{99}Tc found in lobsters in the Irish Sea has risen 44-fold since 1993 when British Nuclear Fuels PLC began treating liquid waste previously stored on-site at the nuclear reprocessing plant in Sellafield, Cumbria [7,8].

MARCEL DEKKER, INC.
270 Madison Avenue, New York, New York 10016

In Paducah, and Portsmouth, ME, USA, the groundwater is contaminated with radionuclides. At 90 ng/L, ^{99}Tc is the principal radioactive metal contaminant. In the Hanford Plant, the groundwater is also contaminated with ^{99}Tc. Furthermore, approximately 1800 kg of ^{99}Tc are stored in on-site tanks, which constitute a major long-term problem associated with the storage of Hanford radioactive waste (10). Similar problems may occur at other nuclear reprocessing plants. In view of its importance, the adsorption of Tc is treated separately and in more detail than the other elements discussed here.

Once the performance of the adsorbent has been understood when applied to solutions of radionuclides in the laboratory-prepared samples, it is hoped that samples of groundwater and samples from storage tanks from nuclear installations can be treated.

In previous work on the precipitation of heavy metals by sulfate-reducing bacteria (11–14), many metal ions in solution could be reduced from ppm to ppb levels, and if magnetic ions were present, their precipitates onto the bacterial cell wall could make the microorganism sufficiently magnetic for removal from the suspension by high-gradient magnetic separation (HGMS) (15–18). A wide range of metal ions were treated with HGMS, such as Ag, Hg, Pb, Cu, Zn, Sb, Mn, Fe, As, Ni, Sn, Al, and other metals, such as Rh, Au, Ru, Pd, Os, Pt, Cr, were also removed. Many of the metals removed do not form insoluble sulfides but were removed when iron sulfide was produced. Watson and Ellwood (14) concluded that the bacteria-produced iron sulfide was acting as an adsorbent for a wide range of heavy metals, including many not normally precipitated as sulfides. Typically the metal ion concentration was reduced from 10 ppm to a few ppb and the capacity for heavy metals was 200–400 mg per g of adsorbent (2). Extended X-ray absorption fine-structure spectroscopy (EXAFS) studies showed that many of the metal ions were chemisorbed (2). Also EXAFS data revealed that the structure of this iron sulfide material does not precisely match any known crystal structure of iron sulfide. The best fits were based on the crystal structure of $Fe_{1-x}S$ obtained by Keller-Besrest and Collin (19). In the best-fit region, with $0 < x < 0.125$, where the lattice parameters depend upon x, the structures are hexagonal of the Ni-As type. In this structure, the Fe atoms are located in sites with octahedral symmetry. This is consistent with the shape of the K X-ray absorption edge (20).

These iron sulfides were only weakly magnetic and if they were to be used as adsorbents on a large scale, the cost of recovering them from suspension could be considerably reduced by making them strongly magnetic. To accomplish the task of making large quantities of strongly magnetic iron sulfide using sulfate-reducing bacteria, Watson, Ellwood, and Duggleby invented a new method (1).

Although the structural properties of this material have been published in detail (21,22), it is appropriate to briefly review the structure of the strongly mag-

MARCEL DEKKER, INC.
270 Madison Avenue, New York, New York 10016

netic iron sulfide because it is pertinent to the adsorption of ions by this material. Finally, a number of important technological aspects of this work are discussed.

PREPARATION AND PROPERTIES OF STRONGLY MAGNETIC IRON SULFIDE

Preparation of Strongly Magnetic Iron Sulfide

As was discussed in the introduction, weakly magnetic iron sulfide adsorbents for heavy metals were produced using sulfate-reducing bacteria grown with a medium containing excess iron in a chemostat. However, in the iron sulfide system, in addition to weakly magnetic phases with the Ni-As structure, strongly magnetic materials were found (23), namely, pyrrhotite (Fe_7S_8), in which ordered vacancies (24) produce a ferrimagnetic monoclinic structure (its saturation magnetization value of 0.1 T is about one-fifth that of nickel), and greigite (Fe_3S_4) (25), which is a strongly ferrimagnetic material. This material has a spinel structure and a saturation magnetization of approximately 0.43 T (26). Therefore, to improve the magnetic properties, the microorganisms need to produce a high percentage of either Fe_7S_8 or Fe_3S_4.

Through a novel method (1,27), progress toward the production of a more magnetic product was achieved in 2 steps. First, the output from the chemostat was treated by magnetic separation to concentrate the strongly magnetic particles of iron sulfide together with the microorganisms in intimate contact with the particles, and second, to feed this strongly magnetic fraction and the attendant microorganisms back to the chemostat or use them to inoculate a new chemostat. Using this method, the low percentage of strongly magnetic fraction was increased to greater than 80% in a period of 3 months. At these larger magnetic concentrations, the inocula taken from the chemostat can be used to produce a consistent source of strongly magnetic iron sulfide.

The magnetic mineral was separated from the chemostat output by HGMS (15–18) in a background of an applied 1-T magnetic field.

The Structural and Magnetic Properties of the Strongly Magnetic Iron Sulfide

The structural properties of the magnetic iron sulfide material have been examined in detail using transmission electron microscopy (TEM), surface area measurements, magnetic measurements, EXAFS, and X-ray absorption near edge structure (XANES) spectroscopy at Daresbury and neutron scattering at the ISIS facility of the Rutherford-Appleton Laboratory (21,22).

MARCEL DEKKER, INC.
270 Madison Avenue, New York, New York 10016

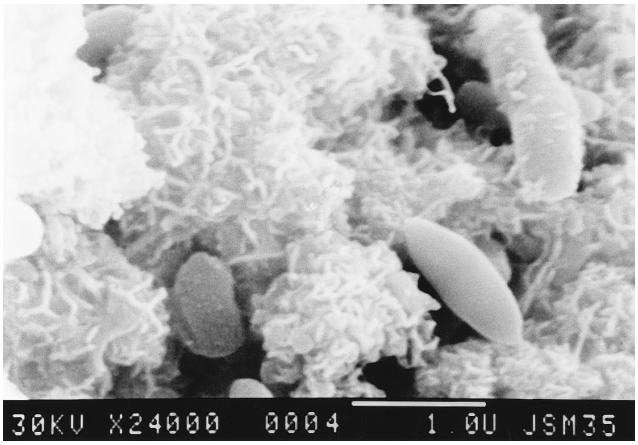

Figure 1. A scanning electron microscope micrograph of iron sulfide adsorbent produced by sulfate-reducing microorganisms. The bacterium in the top-right corner is coated with a finely divided iron sulfide precipitate. Another SRB can be seen in an "end-on view" left-of-center near the bottom of the picture. The smooth microorganism toward the bottom right-hand corner is not an SRB. The scale bar at the bottom of the plate is 2 μm.

Figure 1 shows a scanning electron microscope micrograph of iron sulfide adsorbent produced by sulfate-reducing microorganisms. The SRB in the top-right corner is coated with a finely divided iron sulfide precipitate. Another SRB can be seen in an "end-on view" left-of-center near the bottom of the image. The bacteria are approximately 0.8 μm in diameter and have a length of approximately 4 to 5 μm. The scale bar at the bottom of the figure is 2 μm. The smooth microorganism toward the bottom right-hand corner is not an SRB. The layer of precipitated, finely divided iron sulfide seen around the surface of the bacterium can become detached from the surface of the bacterium and this material, together with the microorganisms that produce it, collect in the bottom of the bioreactor. The bacterium continues to metabolize with the iron sulfide coating indicting that the material forms an open structure through which nutrients can easily flow. This openness is very important when the material is used as an adsorbent because it ensures the rapid uptake of the adsorbate.

Higher magnification reveals that the sample of magnetic iron sulfide consists of very small, irregular particles or clusters of particles, some of which were identified as greigite. The vast majority appears entirely featureless with no clear grain boundary or distinctive morphology. However, a few areas produce weak, diffuse, continuous, or spotty powder-type ring (approximately 3×10^{-2} μm^2) diffraction patterns, indicating a poor degree of crystallinity with very small crystalline domains randomly oriented within the selected area. The lattice spacing of

these rings is consistent with greigite (25,28), but the pattern is very weak and incomplete, so unequivocal identification as greigite is difficult.

The superimposed selected area diffraction patterns (hexagonal array of spots and diffuse rings) suggest that the sulfide probably consists of an intimate mixture of poorly formed greigite and mackinawite (21,22).

Surface Area Measurements

The surface area of the freeze-dried material was measured using the Brunauer, Emmett, Teller (BET) method (29) and was determined to be 18.4 m^2/g. However, based on EXAFS data to determine the surface area occupied per adsorbed atom and the observed adsorption of Cd and Cu, the estimated surface area of the wet adsorbent material was determined to be a few hundred square meters per gram (21). This was also confirmed by neutron scattering measurements, which showed considerable scattering from 2-nm objects from inside the material (22).

Magnetic Properties of the Iron Sulfide

The iron sulfide was largely paramagnetic at 290 K with a small hysteresis and an average magnetic susceptibility, $\chi = 7 \times 10^{-4}$. After the large particles, assumed to be greigite, had been saturated, the magnetization became linear with the applied field showing no saturation up to the maximum of 12.5 T. At 290 K the material is largely paramagnetic, so the spins are largely independent due to disorder in the system, and together with thermal effects, they weaken the spin-spin interaction. If a Bohr magneton number of 2.2 per formula weight (26) and a spin density similar to greigite apply to the iron sulfide, the strongly magnetic material presumably contained approximately 20% of disordered greigite and the remainder was disordered mackinawite.

The samples were cooled to 5 K in an applied field of 5 T, and then the field was switched off and the trapped flux was measured as a function of temperature from 5 to 290 K. These flux measurements were used to estimate the sample surface area as 190 m^2/g. Perhaps if the sample had been cooled to a much lower temperature than 5 K, the estimate of the surface area would have been much higher (21,22).

X-ray Studies

The XANES profile and the EXAFS-fitting parameters clearly show that the Fe was mainly tetrahedrally coordinated. These results are consistent with a mixture of mackinawite and greigite that is suggested by electron diffraction data. Fe in mackinawite is completely tetrahedrally coordinated, whereas in greigite only one-third of Fe is in tetrahedral coordination (20). Greigite is strongly magnetic,

whereas mackinawite is weakly paramagnetic, indicating that a substantial fraction of the material is greigite. As discussed above, the magnetic properties at 290 K suggest that approximately 20% of the sample is greigite.

Discussion of the Structural Aspects of the Material

A plausible explanation based on the magnetic measurements, the stability against oxidation even in the presence of gaseous oxygen, and the neutron scattering data suggest that during the freeze-drying process, the material collapses, forming a porous material composed of small magnetic particles of iron sulfide 2–4 nm in diameter with holes between the particles of average diameter of approximately 2 nm. The surface area of undamaged material would be closer to 500 m^2/g. As mentioned above, the surface area of the freeze-dried material was measured by the BET method (29) as 18.4 m^2/g. This is less than the area estimates of the material prior to freeze-drying (approximately 500 m^2/g) as determined from adsorption of heavy metals (2) and estimated from TEM pictures (14). It is also lower than the measurements obtained from the trapped magnetism as a function of temperature and from neutron scattering measurements described above. The BET surface area measurements of 18.4 m^2/g indicate that most of the 2-nm pores are inaccessible to the nitrogen gas used in the BET method. However, the material that has not been freeze-dried is in the form of nanoparticles consisting of a mixture of disordered greigite and mackinawite, which provides a large surface area onto which the metal ions adsorb. The weakly magnetic materials have been shown to adsorb a wide range of heavy metals (2), and from the adsorption of these metals, the surface area can be estimated at 500 m^2/g. Typically the metal ion concentration was reduced from 10 ppm to a few parts per billion when weakly magnetic materials were used as adsorbents (2). The capacity for heavy metals was 200–400 mg per g of adsorbent. EXAFS studies (2) revealed that many of the metal ions were chemisorbed. The ability of heavy metals to be chemisorbed indicates that residual levels in solution may be reduced to extremely low values and the uptake by the adsorbent at low concentration can be high. The study of the adsorption of materials at these low concentrations is best done with radionuclides.

ADSORPTION OF CATIONS BY THE STRONGLY MAGNETIC IRON SULFIDE MATERIAL

Introduction and Experimental Protocols

Adsorption studies using Cu and Cd with initial metal ion concentrations of 10 ppm gave similar results to the studies reported previously using the weakly magnetic iron sulfide (2). In the work reported here on the use of the strongly magnetic material, the use of radioactive isotopes allowed studies of the adsorp-

tion process for metal-ion concentration levels many orders of magnitude lower than those used in previous work. Radiotracer experiments were undertaken using calibrated solutions of ^{241}Am, ^{109}Cd, ^{139}Ce, ^{57}Co, ^{60}Co, ^{137}Cs, ^{203}Hg, ^{54}Mn, ^{113}Sn, ^{85}Sr, ^{88}Y, and ^{65}Zn. These solutions of radionuclides were supplied by Nycomed et, Amersham International, Buckinghamshire, UK, which certifies that the solution concentrations to $\pm$ 2%; however, in the experiments the concentrations were measured directly. All the above isotopes are γ-ray emitters. As a result, a γ-ray spectrometer was needed to detect changes in activity. Amersham International also supplied solutions of individual radionuclides of ^{63}Ni and ^{99}Tc as TcO_4^-. The Pu solution containing the isotope ratio ^{240}Pu/^{239}Pu $\approx$ 0.26 was obtained from an acid leach of Irish Sea sediment. The analysis of these isotopes required the use of a liquid scintillation counter. All the vials and containers used were acid washed in 2% Spectrosol HNO_3 for 24 hours and then washed in Milli-Q high-purity water prior to use. Metal uptake experiments were undertaken in 30 mL vials (Sterilin, acid washed) that each contained deoxygenated distilled water obtained by passing nitrogen gas through the water for 30 minutes prior to the addition of a small, accurately measured volume of the radionuclides together with 0.048g/L, 0.481g/L, or 4.81 g/L of adsorbent (dry weight). A blank vial, containing no adsorbent, was used for calibration of the solution and to check for nonspecific sorption or other loss mechanisms.

Table 1. Percentage Radioactivity from

						Wet
Gamma Detector		Am	Cd	Ce	Co	Co
Isotope Mass		241	109	139	57	60
Initial activity (Eq/mL)		1.23 ± 0.025	6.93 ± 0.14	0.14 ± 0.003	0.26 ± 0.005	1.25 ± 0.025
Adsorbent (mg/L)	Time (h)					% Activity
	1	9.7 ± 2.1	n.a	0	83.4 ± 10.9	95.1 ± 11.6
	2	6.1 ± 1.4	7.9 ± 3.1	0	82.9 ± 9.5	91.5 ± 10.0
0.048	3	0	12.6 ± 4.2	0	80.8 ± 10.7	90.6 ± 11.2
	5	0	11.2 ± 3.0	0	77.4 ± 9.7	88.2 ± 9.7
	6.5	0	10.3 ± 3.6	0	76.2 ± 9.7	86.4 ± 10.1
	1	0	0	0	20.5 ± 5.0	19.2 ± 4.2
	2	0	0	0	10.5 ± 2.6	9.8 ± 2.2
0.481	3	0	0	0	7.2 ± 2.1	5.7 ± 1.3
	5	0	0	0	n.a.	0
	6.5	0	0	0	4.6 ± 2.3	0
	1	0	0	0	0	0
	2	0	0	0	0	0
4.812	3	0	0	0	0	0
	5	0	0	0	0	0
	6.5	0	0	0	0	0

n.a. Data unavailable.

MARCEL DEKKER, INC.
270 Madison Avenue, New York, New York 10016

During the metal uptake experiments the vials were shaken and turned over every 30 minutes to ensure a homogeneous mix of solution and adsorbent. After the time required for adsorption, 10 mL of solution was filtered through a disposable 0.22 μm polytetrafluoroethylene (Gelman Scientific) filter. The first 2 mL through the filter were discarded to allow for removal of Spectrosol methanol, which had been used to prime the hydrophobic filter. Seven milliliters of solution were collected into a cleaned 7-mL acid-washed Bijou bottle (Sterilin). The samples were then acidified with Spectrosol HNO_3 to 2% to maintain their stability until measurement. This procedure was adopted for the material that is presented in Tables 1, 2, 4, 7(a), and 7(b). For the materials identified in Tables 3, 5, and 6, the containers were prepared in the same way but the samples were not acidified by HNO_3.

The wet adsorbent was in the form of a slurry containing 15% solids (dry weight) and dispersed ultrasonically before addition to the solution. The freeze-dried adsorbent was added as a powder.

Experimental Results for the Adsorption of Cations

In Table 1 the results are presented for a solution containing ^{241}Am, ^{109}Cd, ^{139}Ce, ^{57}Co, ^{60}Co, ^{137}Cs, ^{203}Hg, ^{54}Mn, ^{113}Sn, ^{85}Sr, ^{88}Y, and ^{65}Zn in which the per-

Select Radionuclides by Adsorbent Added and Time

Adsorbent						
Cs	Hg	Mn	Sn	Sr	Y	Zn
137	203	54	113	85	88	65
1.415 ± 0.028	0.65 ± 0.013	1.24 ± 0.025	0.19 ± 0.004	0.52 ± 0.01	1.242 ± 0.025	0.193 ± 0.00
Remaining in Solution						
96.9 ± 12.1	0	92.4 ± 3.7	0	91.3 ± 19.5	10.6 ± 4	48.2 ± 8.2
90.8 ± 10.3	0	92.7 ± 3.3	0	92.2 ± 16.9	8.2 ± 2.6	45.1 ± 6.3
101.6 ± 12.2	0	94.7 ± 3.7	0	92.8 ± 19.2	0	33.7 ± 6.9
95.0 ± 10.8	0	89.2 ± 3.1	0	83.4 ± 15.4	0	23.9 ± 5.0
96.1 ± 11.4	0	93.2 ± 3.4	0	85.6 ± 22.9	0	19.4 ± 4.5
27.4 ± 5.4	0	57.8 ± 2.6	0	94.4 ± 19.0	0	0
23.6 ± 4.4	0	50.8 ± 2.0	0	92.0 ± 16.0	0	0
15.4 ± 2.4	0	46.8 ± 1.7	0	79.0 ± 14.4	0	0
28.1 ± 4.4	0	27.2 ± 1.4	0	85.3 ± 15.5	0	0
20.6 ± 4.0	0	27.4 ± 1.6	0	87.5 ± 17.6	0	0
0	0	14.8 ± 1.2	0	67.1 ± 14.8	0	0
0	0	9.9 ± 0.3	0	64.1 ± 9.8	0	0
0	0	25.7 ± 1.2	0	45.2 ± 9.2	0	0
0	0	7.5 ± 0.7	0	54.3 ± 16.8	0	0
0	0	8.2 ± 0.6	0	58.9 ± 12.7	0	0

MARCEL DEKKER, INC.
270 Madison Avenue, New York, New York 10016

centage of the activity remaining in solution is shown versus time for 0.048, 0.481, and 4.812 g/L adsorbent added to the solution. The error bars are 2 standard deviations of the measurements. In each case, the percentage activity remaining in solution was time-dependent for less than 1 hour, which means that at these metal ion concentrations, the uptake was more rapid than observed previously when higher initial ion concentrations were studied (2). Zeros in the table indicate that the activity was reduced to background, and n.a. indicates that data were unavailable. The results show that Am, Ce, Hg, Sn, and Y were strongly adsorbed with the smallest adsorbent addition of 0.048 g/L. Cd, Co, and Zn were strongly adsorbed by the addition of 0.481 g/L of the adsorbent. Cs and Mn required 4.81 g/L for strong adsorption; however, a small but significant amount of Mn remained in solution. Sr was adsorbed less strongly than any of the other metal ions measured. The percentage of ^{85}Sr activity was reduced 50–60% with the addition of 4.81 g/L of adsorbent. A noticeable feature of all the results in Table 1 is that the percentage activity remaining in solution showed little time dependence and was fairly constant after 1 hour; the activity only appears to depend on the amount of adsorbent added.

Table 2 shows the percentage of radionuclides ^{63}Ni and a mixture of ^{240}Pu and ^{239}Pu that remained in solution in contact with various amounts of the strongly magnetic adsorbent for various times. Ni is significantly and time-dependently adsorbed with 0.048 g/L. However, addition of 0.48 g/L and 4.8 g/L produced little difference in the results, 1–2% of Ni remained in solution. Pu uptake was strong; the activity in solution was reduced to background by the addition of 0.481 g/L and 4.812 g/L of the adsorbent.

ADSORPTION TO THE WET ADSORBENT IN THE PRESENCE OF SODIUM CITRATE

A number of adsorption experiments were carried out in the presence of sodium citrate to discover if the adsorptivity of the radionuclides changed relative to each other in the presence of a complexing agent. The addition of citrate helps to prevent precipitation of hydrolyzable metals. Such information could lead to processes in which the various isotopes could be physically separated from each other.

The citrate solution was produced by adding 3.32 g of sodium citrate to 7 mL of heavy metal solution. The solution was stirred until the sodium citrate had completely dissolved, then the adsorbent was added while the solution was stirred under an atmosphere of nitrogen gas. The results of the metal uptake are shown in Table 3. In the presence of sodium citrate only Cd and Hg were strongly adsorbed; with 0.48 g/L of adsorbent, Cs was adsorbed to background; Sn, Ni, and Zn showed weak adsorption.

MARCEL DEKKER, INC.
270 Madison Avenue, New York, New York 10016

Table 2. Percentage Radioactivity from ^{63}Ni and ^{240}Pu/^{239}Pu by Adsorbent and Time

Liquid Scintillator Detector				Wet Adsorbent	
			Ni		Pu
Isotope Mass			63		240/239
Initial activity (Bq/mL)			330 ± 7		3.37 ± 0.06
Adsorbent (g/L)	Time (h)	Vol (mL)	% Activity Remaining in Solution	Vol (mL)	% Activity Remaining in Solution
0.048	1	6.61	31.3 ± 2.2	n.a.	n.a.
	2	5.9	22.6 ± 1.6	n.a.	n.a.
	3	0.9	25.2 ± 2.1	n.a.	n.a.
	5	5.84	19.2 ± 1.4	n.a.	n.a.
	6.5	5.73	16.7 ± 1.2	n.a.	n.a.
0.481	1	6.11	9.5 ± 0.7	3.16	0.8 ± 1.5
	2	6.14	2.1 ± 0.2	3.46	0.5 ± 1.5
	3	5.57	2.6 ± 0.2	1.92	–0.2 ± 1.5
	5	6.38	1.1 ± 0.1	2.99	–0.4 ± 1.6
	6.5	5.93	0.9 ± 0.1	n.a.	n.a.
	7	n.a.	n.a.	4.69	0.8 ± 1.5
4.812	1	5.35	1.1 ± 0.1	6.04	0.8 ± 2.8
	2	5.93	1.5 + 0.2	6.19	–1.0 ± 2.6
	3	5.57	1.5 ± 0.2	5.89	–1.0 ± 4.6
	5	4.25	1.3 ± 0.1	5.55	–1.5 ± 3.0
	6.5	5	1.3 ± 0.1	n.a.	n.a.
	7	n.a.	n.a.	5.87	1.4 ± 1.4

n.a. Data unavailable.

Adsorption to the Freeze-Dried Material

The stability of the adsorbent in air can be greatly improved by freeze-drying it. A freeze-dried sample left in air on the open bench for a period of at least 18 months showed no change in its magnetic properties and no visible signs of oxidation. This property has important implications for the use of the material as a practical adsorbent. Experiments were performed using the same starting solutions as for studies with the wet adsorbent containing ^{241}Am, ^{109}Cd, ^{139}Ce, ^{57}Co, ^{60}Co, ^{137}Cs, ^{203}Hg, ^{54}Mn, ^{63}Ni. ^{113}Sn, ^{85}Sr, ^{88}Y, and ^{65}Zn. The results were not as extensive as for the wet adsorbent; only additions of 0.048 g/L and 0.48 g/L were used.

Table 4 shows that the activity of metals Am, Cd, Ce, Sn, Y, and Zn were reduced to background, and Hg was strongly adsorbed with the addition of 0.48

Table 3. Percentage Radio Activity from Select Radionuclides

	Time (h)	^{241}Am	^{109}Cd	^{139}Ce	^{57}Co	^{60}Co
Initial activity (Bq/mL)	0	1.339	6.98	0.151	0.261	1.305
Wt. of Adsorbent (g/L)						% Remaining
0.048	2	96.8	8.6	93.40	92.72	91.18
0.048	3	113	0	114.0	115	107.0
0.048	5	115	0	113.20	113	108.1
0.48	2	n.a.	n.a.	n.a.	n.a.	n.a.
0.48	3	113	0	111.30	1.06	102.8
0.48	5	n.a.	n.a.	n.a.	n.a.	n.a.

n.a. Data unavailable.

g/L. Overall, the results for the freeze-dried material at the adsorbent additions used were similar to those for the wet adsorbent. The similarity in results at low metal ion concentration indicates that the binding mechanisms to the adsorbent are similar; however, their large differences in surface area likely results in very different total-binding capacities. This is an important area for further investigation.

Table 4. Percentage Radio Activity from Select

	Time (h)	^{241}Am	^{109}Cd	^{139}Ce	^{57}Co	^{60}Co
Initial activity (Bq/mL)	0	1.228	6.93	0.14	0.3	1.3
Wt. of Adsorbent (g/L)						% Remaining
0.048	2	0	n.a.	0	44.3	66.9
0.048	3	0	16.4	0	53.8	55.5
0.048	4	0	3.8	0	63.4	67.5
0.048	5	0	9.5	0	71.8	74.9
0.048	6.5	0	5.1	0	61.8	67.4
0.48	2	0	0	0	38.2	40.1
0.48	3	0	0	0	32.4	33.3
0.48	4	0	0	0	22.9	23.9
0.48	5	0	0	0	23.7	24.8
0.48	6.5	0	0	0	26.0	25.4

n.a. Data unavailable.

MARCEL DEKKER, INC.
270 Madison Avenue, New York, New York 10016

by Adsorbent and Time in Presence of Sodium Citrate

^{137}Cs	^{203}Hg	^{54}Mn	^{113}Sn	^{85}Sr	^{88}Y	^{65}Zn	^{63}Ni
1.405	0.176	17.2	0.728	0.5	1.3	0.208	330
in Solution							
45.7	15.9	93.7	87.91	98.1	91	76.92	n.a.
47.0	0	110.9	104.1	113.3	109.5	88.46	n.a.
26.8	0	110	105.1	111.2	110.5	93.26	81.6
n.a.	n.a.	n.a.	n.a.	n.a.	n.a.	n.a.	64.2
0	0	107.7	55.76	76	106.6	83.65	46.7
n.a.	n.a.	n.a.	n.a.	n.a.	n.a.	n.a.	66.5

Adsorption to the Freeze-Dried Material in the Presence of Sodium Citrate

The results for the adsorption of ^{241}Am, ^{109}Cd, ^{139}Ce, ^{57}Co, ^{60}Co, ^{137}Cs, ^{203}Hg, ^{54}Mn,^{63}Ni, ^{113}Sn, ^{85}Sr, ^{88}Y, and ^{65}Zn with freeze-dried adsorbent and

Radionuclides by Freeze-Dried Adsorbent and Time

^{137}Cs	^{203}Hg	^{54}Mn	^{113}Sn	^{85}Sr	^{88}Y	^{65}Zn	^{63}Ni
1.4	0.173	17.3	0.649	0.5	1.2	0.193	330
in Solution							
67.1	8.7	85	0	92.9	1.1	0	63.8
68.0	9.25	79.3	0	89	1.4	0	61.9
67.1	n.a.	82.7	0	97.1	0	0	60.4
65.0	7.51	86.5	0	87.7	1.7	17.6	63.4
63.5	10.98	84.8	0	94.6	0	0	61.1
54.0	7.51	73	0	87.5	1.1	0	30.9
57.4	10.98	69.1	0	87.3	0	0	29
62.5	9.25	59.4	0	88.7	4.8	0	n.a.
52.2	7.51	64	0	81.7	0	0	n.a.
55.4	0	64.5	0	86.3	0	0	n.a.

MARCEL DEKKER, INC.
270 Madison Avenue, New York, New York 10016

Table 5. Percentage Radio Activity from Select Radionuclides by

	Time (h)	^{241}Am	^{109}Cd	^{139}Ce	^{57}Co	^{60}Co
Initial activity (Bq/mL)	0	1.339	6.98	0.151	0.261	1.305
Wt. of Adsorbent (g/L)						% Remaining
0.048	2	103	0	0	93.9	94.3
0.048	3	99	0	0	94.7	89.9
0.048	4	105	0	0	88.5	97.9
0.048	5	98	0	0	92.0	96.2
0.048	6.5	97	0	0	96.9	88.4
0.48	2	n.a.	n.a.	n.a.	n.a.	n.a.
0.48	3	n.a.	n.a.	n.a.	n.a.	n.a.
0.48	4	n.a.	n.a.	n.a.	n.a.	n.a.
0.48	5	n.a.	n.a.	n.a.	n.a.	n.a.
0.48	6.5	n.a.	n.a.	n.a.	n.a.	n.a.

n.a. Data unavailable.

sodium citrate are shown in Table 5. Although some Cs, Ni, and Zn isotopes were adsorbed, only Cd, Ce, and Hg were strongly adsorbed. This result is in contrast to the wet adsorbent with sodium citrate (Table 3), in which Cd and Hg were strongly adsorbed and some Cs was adsorbed with the addition of 0.048 g/L and more completely adsorption with the addition of 0.48 g/L. The most remarkable difference is found for Ce, which was strongly adsorbed by the wet adsorbent without citrate and was also adsorbed with the freeze-dried material, with and without citrate, but was not adsorbed on the wet adsorbent with citrate. These results are not sufficiently detailed to form a clear picture, but they raise interesting questions to be answered by future work. One question raised, which was preliminarily examined, is whether citrate solutions can be used to wash the adsorbent to separate the metals differentially.

Treatment of the Wet Adsorbent with a Citrate Wash to Remove Adsorbed Metal Ions

Forty-eight milligrams (dry weight) of strongly magnetic wet adsorbent were added to 100 mL of the solution that contained ^{241}Am, ^{109}Cd, ^{139}Ce, ^{57}Co, ^{137}Cs, ^{203}Hg, ^{113}Sn, ^{85}Sr, ^{88}Y, and ^{65}Zn, and the suspension was stirred for 6 hours under a nitrogen blanket. Then, the concentrations remaining in solution were

MARCEL DEKKER, INC.
270 Madison Avenue, New York, New York 10016

Freeze-Dried Adsorbent and Time in Presence of Sodium Citrate

^{137}Cs	^{203}Hg	^{54}Mn	^{113}Sn	^{85}Sr	^{88}Y	^{65}Zn	^{63}Ni
1.405	0.176	17.2	0.728	0.5	1.3	0.208	330
in Solution							
87.1	0	97.7	90.7	97.9	91.2	93.3	71.9
87.0	0	94.3	93.4	90.2	92.4	77.9	69.2
92.4	0	94.5	89.4	83	97.4	82.2	67.9
94.0	0	92.7	87.4	95.3	89.2	88	69.8
92.6	0	94.3	90.9	91.6	93.8	61.5	33.3
n.a.	n.a.	n.a.	n.a.	n.a.	n.a.	n.a.	41.5
n.a.	n.a.	n.a.	n.a.	n.a.	n.a.	n.a.	40.7
n.a.	n.a.	n.a.	n.a.	n.a.	n.a.	n.a.	n.a.
n.a.	n.a.	n.a.	n.a.	n.a.	n.a.	n.a.	60.1
n.a.	n.a.	n.a.	n.a.	n.a.	n.a.	n.a.	36.2

measured to determine the amount of each isotope adsorbed. The adsorbent was filtered from the suspension and was added to 50 mL of distilled water that was subsequently added to 50 mL of a citrate buffer with pH = 6. The buffer solution consisted of 9.5 mL of 0.1 mol/L citric acid and 40.5 mL of 0.1 mol/L sodium citrate. The radionuclide concentrations recovered into solution by the citrate buffer were monitored as a function of time and the results are presented in Table 6.

Substantial percentages of the adsorbed radionuclides, except Cd and Cs, can be recovered from the adsorbent through the use of the citrate buffer. These are interesting, but preliminary results, that require more research. One of the questions to be answered is whether or not the adsorbent can be reused after the washing process.

Discussion of the Experimental Results for the Adsorption of Cations

The isotopes apparently did not adsorb to the walls of the containers. This is reflected in the results shown in Tables 1 and 2: All the metals having low sulfide solubility products were reduced to low concentrations by small additions of adsorbent, whereas Co, Cs, Mn, and Sr were largely unchanged. However, further reductions in concentrations of these metals can be achieved by increasing the

Table 6. Radionuclide Recovery in

						Wet Adosrbent
Gamma Detector		Am	Cd	Ce	Co	Cs
Isotope Mass		241	109	139	57	137
Initial activity (Bq/mL)		1.23 ± 0.025	6.93 ± 0.14	0.14 ± 0.003	0.26 ± 0.005	1.25 ± 0.025
Uptake after 6 h before addition of citrate (%)		100	100	100		41
Adsorbent (mg/L)	Time (h)					% Activity
	0.25	27.6 ± 2.7	0	39.8 ± 16.8	n.a.	0
	0.5	21.3 ± 5.5	0	n.a.	n.a.	0
0.048	2	25.0 ± 9.7	0	n.a.	n.a.	0
	3	33.4 ± 8.2	0	41.3 ± 13.6	n.a.	0
	4	25.3 ± 11	0	n.a.	n.a.	0
	5	32.4 ± 2.1	0	41 ± 12.3	n.a.	0
	22	29.6 ± 4.3	0	50.3 ± 25.1	n.a.	0
	51	36.5 ± 3.0	0	41.7 ± 18.7	n.a.	0

n.a. Data unavailable.
The citrate buffer was at pH = 6.0 and consisted of 9.5 mL of 0.1 mol/L citric acid 40.5 mL of 0.1 mol/L M sodium

amount of adsorbent added. This dependence on the amount of adsorbent added also indicates that processes such as hydrolysis are not the cause of the reduction in metal ion concentrations. The behavior of Cs is rather surprising, and at present we have no explanation for this result. However, adsorption to the walls of the container is unlikely because the concentration in solution was dependent on the amount of adsorbent added.

The data for Ce are very interesting because Ce^{3+} is often used to model the behavior of Pu and the trivalent actinides, and the results presented here are consistent with this relationship (30,31). A further indication of the reliability of the results is the high correspondence between the two Co isotopes.

In Table 3 the results are presented for the adsorption of metal ions in the presence of a citrate solution that is both a strong metal ligand and a pH buffer. Both of these properties make the citrate a good solubilizing agent, especially for transition metals. Therefore, it is surprising that roughly 40% of the Ni was adsorbed by 0.48 g/L of the adsorbent and that Cs was reduced to background by the addition of 0.48 g/L even in the presence of a high concentration of Na ions. At present, we have no explanation for this and clearly more work needs to be done. Cd^{2+} and Hg^{2+} sulfides have very low solubility and continue to be strongly adsorbed even in the presence of citrate.

Table 4 contains results of applying freeze-dried adsorbent to the same cocktail of metal ions (without Pu) that are presented in Tables 1 and 2. The results are very similar to those shown in Table 2 except for Hg and Cs, which seem

MARCEL DEKKER, INC.
270 Madison Avenue, New York, New York 10016

Solution by Citrate Buffer by Time

Adsorption Followed by a Citrate Wash				
Sr	Hg	Sn	Y	Zn
85	203	113	88	65
1.415 ± 0.028	0.65 ± 0.013	0.19 ± 0.004	1.242 ± 0.025	0.193 ± 0.003
60	35	100	100	100
Recovered into Solution by Citrate Wash				
65.2 ± 15.5	70.1 ± 33.6	20.7 ± 43	25.8 ± 4.3	58.1 ± 6.5
n.a.	n.a.	n.a.	n.a.	47.8 ± 10.7
n.a.	n.a.	n.a.	n.a.	89.1 ± 21
57.1 ± 20.9	65.8 ± 45	18.6 ± 8.0	32.2 ± 4.9	68.7 ± 4.8
n.a.	n.a.	n.a.	n.a.	68.8 ± 21
52.9 ± 13.0	66.7 ± 25	66.7 ± 24.8	35.6 ± 4.1	51.5 ± 3.6
n.a.	n.a.	n.a.	36.0 ± 7.1	27.0 ± 6.8
51.5 ± 13.9	90.6 ± 50	n.a.	41.2 ± 5.2	18.7 ± 4.9

citrate in a 50 mL sample.

to be much less strongly adsorbed, and Zn, which appears to be more strongly adsorbed. The freeze-drying process, in addition to reducing the surface area from 500 to 18 m^2/g, may change the nature of the surface sites particularly affecting the adsorption of Hg and perhaps Cs.

Table 5 shows the adsorption of metal ions to the freeze-dried adsorbent in the presence of the citrate solution. The metal sulfides with low solubility products were strongly adsorbed, and it is curious that Hg was more strongly adsorbed with citrate than without it. A comparison of these results with those from the wet adsorbent in the presence of citrate experiments reveals that Ce is strongly adsorbed to the freeze-dried material but not to the wet adsorbent.

These experiments (Tables 1–5) have demonstrated that the strongly magnetic iron sulfide material is an effective adsorbent for the heavy metals at the low concentrations often encountered in nature and by the nuclear industry.

If the material is to be reused after adsorption, to be useful, the adsorbed metal must be washed off and be produced at a concentration much higher than the original solution. This has been studied here using the citrate buffer, and the results are presented in Table 6. The results show that Cd and Cs remained strongly adsorbed in the citrate buffer for up to 51 hours. The Cd has been shown to be chemisorbed (2), so Cs may also be chemisorbed; this needs further examination using EXAFS.

After 5 hours in contact with citrate, approximately 60% of the adsorbed Zn was recovered into solution, but after 51 hours, 40% of the Zn appears to have

been readsorbed. Because most of the other ions have reached a steady value within 51 hours, substitution of other ions by Zn can be ruled out as a cause for Zn readsorption. This may mean that a partial dissolution of the adsorbent is revealing new surface sites suitable for the adsorption of Zn. These adsorption experiments have revealed many areas requiring further study.

THE ADSORPTION OF THE PERTECHNETATE ION

Introduction

In view of the importance that has been attached to the pertechnetate ion, TcO_4^-, as constituting a major factor in the environmental impact of the nuclear fuel cycle, the adsorption of technetium has been considered more extensively than other heavy metals presented in this paper.

In a report by Bostick and Evans-Brown (32), which will be subsequently discussed in more detail, data were presented on the removal of pertechnetate from solution by the addition of chemically precipitated greigite, Fe_3S_4, in the presence of 2.3 mol/L $NaNO_3$ and achieved an uptake of 0.135 mg per g of greigite. Although this value is small, it gave encouragement that the greigite generated by microorganisms, with a surface area per g approximately 100-fold larger than the chemically precipitated material, would perform considerably better than the chemically precipitated material.

In the work presented here, the adsorption of the pertechnetate ion was considered under a wide range of conditions. The adsorbed ion was examined by EXAFS, and the results of the adsorption studies described were compared with previous work in which other adsorbents had been used.

The results of adsorption by ion exchange resins are often expressed as the coefficient of sorption *Kd*, which is defined as the m/mol of adsorbate adsorbed per gram of adsorbent divided by the m·mol/ml of adsorbate left in solution at equilibrium. However, *Kd* does not seem appropriate when dealing with reductants or with chemisorption, so in this work *Kc* is used and is defined as follows:

$$Kc(\text{mL/g}) = \frac{\left(\begin{array}{c}\text{Initial adsorbate}\\ \text{concentration}\\ \text{m}\cdot\text{mol/L}\end{array} - \begin{array}{c}\text{Final adsorbate}\\ \text{concentration}\\ \text{m}\cdot\text{mol/L}\end{array}\right) \Big/ \begin{array}{c}\text{Adsorbent}\\ \text{concentration}\\ \text{g/L}\end{array}}{\begin{array}{c}\text{Final adsorbate}\\ \text{concentration}\\ \text{m}\cdot\text{mol/L}\end{array}}$$

When the above equation is applied to an ion exchange resin, $Kc = Kd$. *Kd* is the symbol most often used for ion exchange resins.

MARCEL DEKKER, INC.
270 Madison Avenue, New York, New York 10016

Experimental Results on the Adsorption of the Pertechnetate Ion

The containers used in this work were treated as described in the experimental protocol used for the adsorption of positive ions. The wet adsorbent was added as a slurry of approximately 15% solids and except where stated, the slurry was dispersed using ultrasound for approximately 15 minutes.

The adsorption of the Tc, in the form of the pertechnetate ion (TcO_4^-), is shown in Tables 7a and 7b.

As shown in Table 7a, from an initial activity of 485.3 Bq/mL (0.765 μg/mL), the addition of 0.048 g/L of adsorbent produced little effect. However, in a separate experiment, when the adsorbent level was increased to 0.48 g/L, the activity was reduced by 50% in approximately 1.5 to 2.0 hours, which corresponds to an uptake of 0.8 mg Tc per g of adsorbent. With the addition of 4.81 g/L of adsorbent, the activity remaining in solution was less than 1% after less than 1 hour, which corresponds to an uptake of approximately 0.16 mg Tc per g of adsorbent. As will be subsequently discussed, EXAFS studies indicated that the TcO_4^- is chemisorbed by the adsorbent.

Four more experiments were undertaken, the results of which are presented in Table 7b. The first experiment tested the effectiveness of adsorbent that had been in storage, under anaerobic conditions, for approximately 18 months. To a

Table 7a. Percentage Radioactivity from TcO_4^- by Adsorbent and Time

Isotope Mass Initial Activity (Bq/mL)			Wet Adsorbent Tc 99 485.3 ± 10 (0.765 μg/mL)		
Adsorbent (g/L)	Time (h)	Vol (mL)	% Activity Remaining in Solution	Tc Uptake (mg/g)	Kc (mL/g)
0.048	1	6.62	98.88 ± 1.72	0.23 ± 0.23	305 ± 305
	2	6.03	98.80 ± 1.72	0.23 ± 0.23	313 ± 313
	3	5.32	99.39 ± 1.73	0.19 ± 0.19	250 ± 250
	5	6.17	99.62 ± 1.73	0.17 ± 0.17	225 ± 225
	6.5	6.19	100.29 ± 1.74	0.12 ± 0.12	153 ± 153
0.481	1	6.16	65.33 ± 1.28	0.56 ± 0.02	1105 ± 62
	2	6.16	47.10 ± 1.03	0.84 ± 0.02	2337 ± 97
	3	5.99	48.79 ± 1.06	0.81 ± 0.02	2184 ± 93
	5	5.59	62.18 ± 1.24	0.60 ± 0.02	1266 ± 67
	6.5	5.11	59.84 ± 1.21	0.64 ± 0.02	1397 ± 70
4.812	1	5.42	6.77 ± 0.32	0.15 ± 0.34%	2869 ± 145
	2	4.83	1.01 ± 0.10	0.16 ± 0.13%	20570 ± 2060
	3	5.88	1.12 ± 0.10	0.16 ± 0.13%	18500 ± 1670
	5	5.54	1.00 ± 0.09	0.16 ± 0.13%	20740 ± 1886
	6.5	5.13	0.58 ± 0.06	0.16 ± 0.13%	36010 ± 3750

MARCEL DEKKER, INC.
270 Madison Avenue, New York, New York 10016

Table 7b. Summary of Tc Uptake by Adsorbent per Experiment

			Wet Adsorbent Tc		
Adsorbent (g/L)	Time (h)	Vol (mL)	Tc Remaining in Solution (μg/mL)	Tc uptake (mg/g)	Kc (mL)
Untreated after storage for 18 months					
13.333	0	12.0	0.97 ± 0.02	0	0
	17	5.3	0.09 ± 4%	0.07 ± 0.15%	784 ± 4%
The same material as above but treatment in ultrasonic bath for 15 minutes					
13.333	0	12.0	0.97 ± 0.02	0	0
	1	5.32	0.01 ± 0.34%	0.75 ± 0.15%	7560 ± 250
Adsorbent produced for EXAFS-Sample 1 adsorbent in the presence of 2 mol/L NO_3–					
27	0	12.0	250 ± 0.02	0	0
	0.3	5.3	220 ± 0.34%	0.90 ± 0.12	4 ± 0.9
Adsorbent produced for EXAFS—Sample 2 no NO_3– present					
27	0	12.0	250 ± 4	0	0
	0.3	5.02	30 ± 0.34%	8.15 ± 0.06	273 ± 250

12-mL sample containing 11.64 μg of ^{99}Tc (as TcO_4^-) with an activity of 7360 Bq (970 ng/ml) was added 0.16 g (13.333 g/L) of adsorbent. The removal of TcO_4^- was slow; after 17 hours, the activity in solution was 644 ± 25 Bq (10 ng/mL), which amounted to an uptake of 0.066 mg Tc per g of adsorbent. The second experiment was a repeat of the first under the same conditions and using the same quantities, but the adsorbent was dispersed ultrasonically for 15 minutes before being added to the pertechnetate solution. With the sonicated adsorbent, the Tc activity in the solution went from 7360 Bq to background within 1 hour, which corresponds to an uptake of 0.073 mg Tc per g of adsorbent. This experiment amply illustrates the need for properly dispersing the adsorbent to achieve the best Tc uptake.

Two additional experiments were carried out on a concentrated solution of the pertechnetate ion, and the resulting loaded adsorbent materials were used as samples 1 and 2 in the EXAFS studies presented in Figs. 2a, 2b, 3a, and 3b.

First, to simulate the effluent from a nuclear reprocessing plant (32–34), $NaNO_3$ was added to the pertechnetate solution to produce a NO_3^- concentration of 2 mol/L (102 g/L), and 27 g/L of wet adsorbent was added to this solution, which reduced the activity in solution from the initial value of 1.55×10^5 Bq/mL (0.25 mg/mL) to 1.40×10^5 Bq/mL (0.22 mg/mL) in a period of 0.3 hours. This result, as shown in Table 7b, corresponds to an uptake of 0.9 mg per g of adsorbent, whereas for lower pertechnetate ion concentrations (results shown in Table

Marcel Dekker, Inc.
270 Madison Avenue, New York, New York 10016

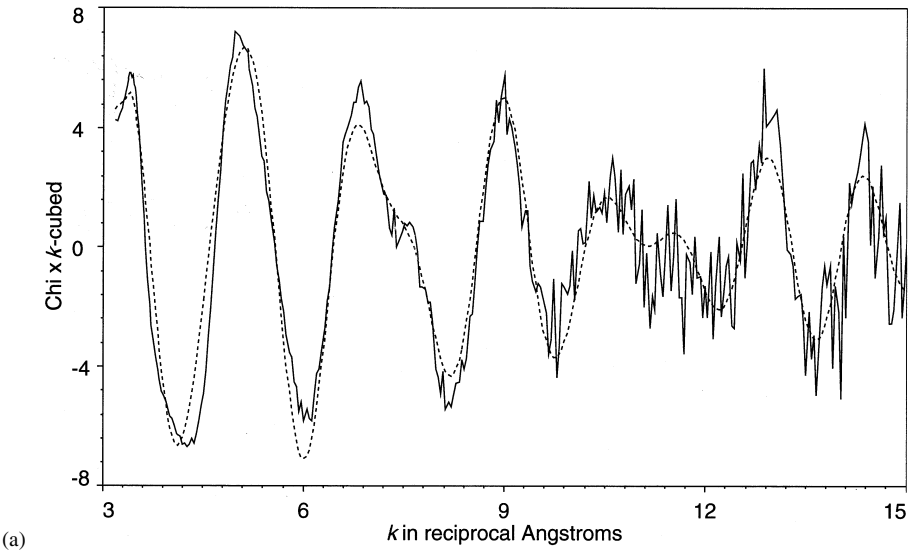

(a)

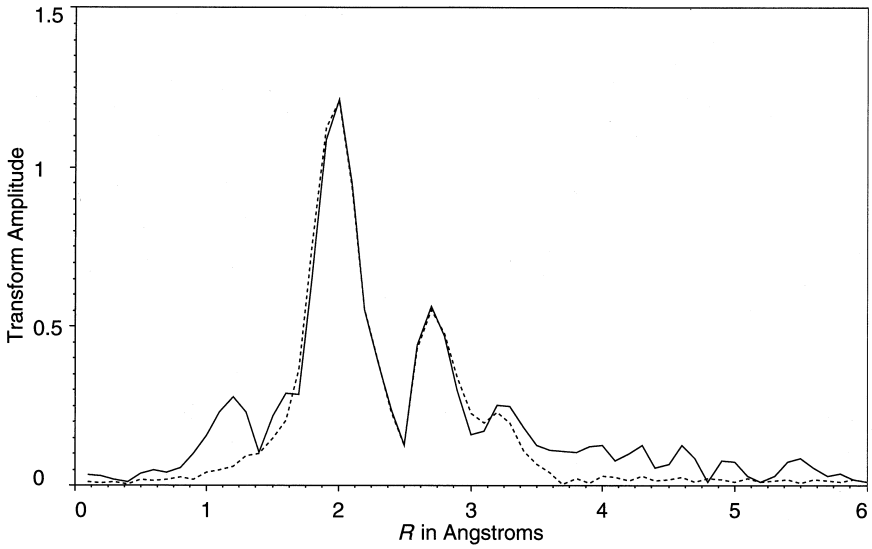

(b)

Figure 2. (a) The k^3-weighted Tc K-edge EXAFS spectrum (solid line) and best fit (broken line) of sample 1, and (b) the corresponding Fourier transforms.

MARCEL DEKKER, INC.
270 Madison Avenue, New York, New York 10016

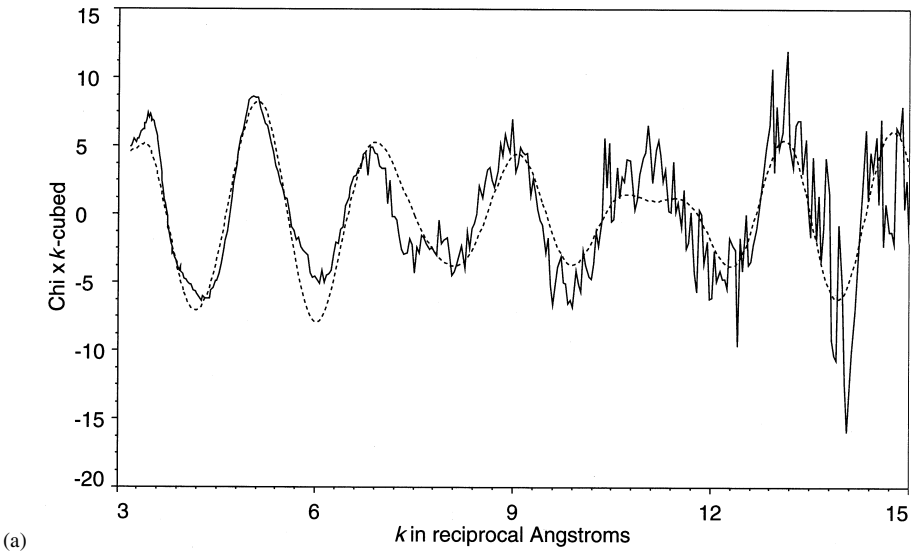

(a)

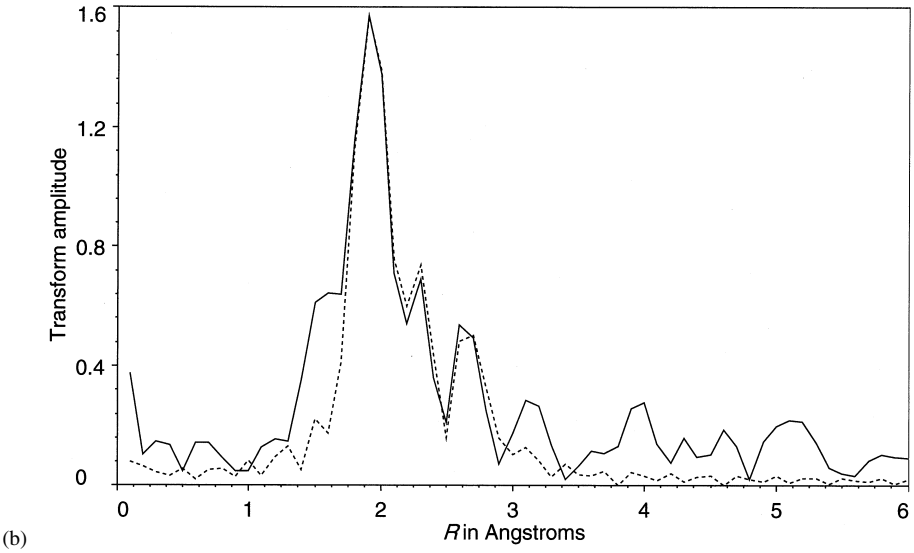

(b)

Figure 3. (a) The k^3-weighted Tc K-edge EXAFS spectrum (solid line) and best fit (broken line) of sample 2, and (b) the corresponding Fourier transforms.

MARCEL DEKKER, INC.
270 Madison Avenue, New York, New York 10016

7a) the maximum uptake per g was 0.84 mg per g. In the EXAFS studies, the resulting loaded adsorbent was designated "sample 1."

Second, 27 g/L of wet adsorbent was added to the solution that contained NO_3^-, which reduced the activity from 1.55×10^5 Bq/mL (0.25 mg/mL) to 1.86×10^4 Bq/mL (0.03 mg/mL) after 0.3 hours and corresponds to a TcO_4^- uptake of 8.15 mg Tc per g of adsorbent, which is considerably higher than the uptake in the presence of NO_3^-. In the EXAFS studies, this loaded adsorbent was designated "sample 2."

The presence of NO_3^- concentrations affected the uptake of the pertechnetate ion; this requires more study particularly because it is pertinent to the removal of pertechnetate ions from nuclear reprocessing plants. However, even in the presence of 2 mol/L NO_3^-, the uptake was still significant at 0.9 mg Tc per g of adsorbent. This illustrates that the NO_3^- ions are in strong competition with the TcO_4^- for adsorption sites. This probably indicates that the uptake of NO_3^- was approximately 4 mg per g of adsorbent. These factors will be subsequently discussed in more detail.

EXTENDED X-RAY ABSORPTION FINE STRUCTURE ON THE TC-LOADED ADSORBENT

Experimental Details

The 2 Tc samples were prepared and loaded into Perspex sample holders with Sellotape windows. Sample 2, containing higher amounts of Tc, was sealed in a Perspex box with Kapton windows and encapsulated in a heat-sealed plastic bag to minimize any risk of contaminating the experimental area. Data were collected at ambient temperature in the fluorescence mode on station 9.2 of the Daresbury Synchrotron Radiation Source that operated at 2 GeV with an average current of 150 mA. A Si (220) double-crystal monochromator was detuned to reject 50% of the incident signal to minimize harmonic contamination. The monochromator angle was calibrated by running an edge scan for a Fe foil. The station was not further calibrated at the Tc edge. Io and It (the initial and the transmitted intensities) were measured using ion chambers filled with a mixture of Ar/He, and the fluorescence signal was collected with a solid state 13-element Canberra detector windowed on the Tc Kα fluorescence signal. Sixteen scans were made at the Tc K-edge for sample 1, and 5 scans were made at the Tc K-edge for sample 2 in the range 200 eV below the edge to 900eV above it.

The isolated EXAFS data were analyzed using EXCURV92 (35), employing the exact spherical wave calculation (36,37). Phase shifts were derived from ab initio calculations using Hedin-Lundqvist potentials and von Barth ground states (38). The theoretical fits were obtained by adding shells of backscattering

MARCEL DEKKER, INC.
270 Madison Avenue, New York, New York 10016

atoms around the central absorber atom and iterating the Fermi energy, E_f, the absorber-scatterer distances, r, and the Debye-Waller factors, $2\sigma^2$, to minimize the sum of the squares of the residuals between the experiment and the theoretical fit. The numbers of scatterers, N, in each shell were chosen as the integer values that gave the best fit. Only shells that made a significant improvement to the R-factor were included in the final fit. The R-factors listed in the tables represent a measure of the goodness of fit defined by the equations:

$$R = \sum_i \left[\frac{1}{\sigma_i}\right] |\text{experiment } (i) - \text{theory } (i)| \times 100\%$$

where

$$\frac{1}{\sigma_i} = \frac{k(i)^3}{\sum_j [k(j)^3] |\text{experiment } (j)|}$$

Experimental Results

Sample 1

Technetium (TcO_4^-) in a 2 mol/L nitrate ion solution was adsorbed onto strongly magnetic iron sulfide derived from sulfate-reducing bacteria. The Fourier transform spectrum of sample 1 shows that several shells were clear. The first shell was best fitted using 4 O atoms at 0.199 nm. The second major shell could be fitted with 2 Fe atoms at 0.271 nm. The fit was significantly improved when a sulfur atom at 0.227 nm was included, and the addition of a second metal shell at 0.300 nm (Fe) or 0.331 nm (Tc) also created a slight improvement. The best fit was with Tc in the second shell. These fits are summarized in Table 8. Figures 2a and 2b show the best fit to the experimental spectrum and the associated Fourier transforms.

Sample 2

Technetium (TcO_4^-) from a nitrate-free solution was adsorbed onto strongly magnetic iron sulfide derived from sulfate-reducing bacteria. The spectrum for sample 2 is very similar to that obtained for sample 1, which contained the lower Tc concentration. The first shell was best fitted using 4 O atoms at 0.199 nm. When a sulfur atom at 0.227 nm was included, the fit was significantly improved, and the third shell could be fitted with 2 Fe atoms at 0.270 nm. The addition of a second metal shell of Tc atoms at 0.323 nm also made a slight improvement in the fit. These fits are summarized in Table 9. Figures 3a and 3b show the best fit to the experimental spectrum and the associated Fourier transforms.

MARCEL DEKKER, INC.
270 Madison Avenue, New York, New York 10016

Table 8. Best Fit of Atoms in Sample 1 Tc Shells

Shell	r(nm)	$2\sigma^2$(nm^2)	R-factor
4 × O	0.199	0.0006	32.1
1 × S	0.227	0.0011	
2 × Fe	0.271	0.0014	
1 × Tc	0.330	0.0012	
4 × O	0.199	0.0006	34.6
1 × S	0.227	0.0010	
2 × Fe	0.271	0.0012	
2 × Tc	0.331	0.0019	
4 × O	0.199	0.0007	35.8
1 × S	0.227	0.0013	
2 × Fe	0.271	0.0013	
2 × Fe	0.300	0.0033	
4 × O	0.199	0.0007	37.6
1 × S	0.227	0.0013	
2 × Fe	0.271	0.0013	
4 × O	0.199	0.0007	40.1
2 × Fe	0.271	0.0014	
4 × O	0.199	0.0007	43.2
4 × Fe	0.270	0.0032	
4 × O	0.200	0.0007	45.1
4 × S	0.286	0.0021	
4 × O	0.200	0.0007	46.4
2 × Tc	0.255	0.0031	
4 × O	0.200	0.0007	47.9
4 × S	0.211	0.0015	61.0

Data based on EXAFS data. r is the distance of the shell from the Tc atom, measured as the distance from the central Tc atom and the Scatterer ± 0.002 nm. 2 σ^2 is the Debye-Waller factor ±20%.

Discussion of the Experimental Results

The experimental results show that the uptake of the pertechnetate ion by the adsorbent is very rapid and high, even in the presence of 2 mol/L NO_3^-, when compared with ion exchange resins.

EXAFS data show that the pertechnetate ion reacts chemically with the surface of the adsorbent and that Tc remains chemisorbed at the surface by a Tc-S bond. They also show other strong interactions between Tc and Fe.

In these samples, the technetium was coordinated by 4 oxygen at 0.197 (sample 1) and 0.199 nm (sample 2); these distances are significantly longer than the Tc-O bond length of 0.1703 nm in the pertechnetate anion (39) and are con-

MARCEL DEKKER, INC.
270 Madison Avenue, New York, New York 10016

Table 9. Best Fit of Atoms in Sample Shells

Shell	r(nm)	$2\sigma^2$(nm^2)	R-factor
4 × O	0.197	0.0002	48.2
1 × S	0.227	0.0001	
1 × Fe	0.267	0.0007	
1 × Tc	0.323	0.0010	
4 × O	0.197	0.0002	49.1
1 × S	0.227	0.0001	
1 × Fe	0.267	0.0006	
1 × Fe	0.306	0.0027	
4 × O	0.197	0.0002	48.8
1 × S	0.227	0.0001	
1 × Fe	0.267	0.0007	
4 × O	0.197	0.0002	49.3
1 × S	0.227	0.0001	
2 × Fe	0.267	0.0014	
4 × O	0.196	0.0002	52.4
1 × S	0.227	0.0001	
4 × O	0.197	0.0001	54.4
2 × S	0.227	0.0007	
4 × O	0.197	0.0002	60.0
4 × S	0.219	0.0021	78.4

Data based on EXAFS data. r is the distance of the shell from the Tc atom, measured as the distance from the central Tc atom and the Scatterer + 0.002 nm. 2 σ^2 is the Debye-Waller factor ±20%.

sistent with either a chemical reduction of the technetium or an increase in the coordination number or both. The view that the Tc has been chemically reduced is consistent with the EXAFS studies on TcO_2 by Almahamid and coworkers (40) who found a Tc-O bond length of 0.198 nm. A significant Tc-S interaction at 0.227 nm existed in both samples, showing that when the Tc is adsorbed on the surface a Tc-S bond is formed. A significant Tc-Fe interaction at 0.270 nm is suggested. The short distance implies a doubly bridged (1 × S + 1 × O, 2 × O, or 2 × S) system. A further metal shell is evident at approximately 0.3 nm. Both samples can be fitted with either Fe at 0.300–0.306 nm or Tc at 0.323–0.330 nm, but in each case the fit with Tc scatterers gives the lower R-factor, and in sample 2, the 4-shell fit with the shell of Fe scatterers at 0.306 nm was worse than the 3-shell fit without them.

Haines, Owen, and Vandergraaf (41) confirmed that TcO_4^- can be reduced at the surface of magnetite (Fe_3O_4). They used Fourier transform infrared spectroscopy to show conclusively that the reaction between TcO_4^- and Fe_3O_4 at room

temperature occurs via a surface reduction of TcO_4^- to TcO_2 with the latter being precipitated at the Fe_3O_4 surface. Fe_3S_4 and Fe_3O_4 are isomorphous.

The coordination of Tc on the adsorbent surface was very similar in samples 1 and 2, which strongly suggests that the role of NO_3^- is simply to compete with the TcO_4^- for the same sites on the adsorbent. As shown in Table 7b, when 27 g/L of adsorbent were added to 250 mg/L of Tc in the presence of 2 mol/L NO_3^-, the ratio of NO_3^- to Tc was 800 and the uptake of Tc was approximately 0.9 mg/g of adsorbent. In the absence of NO_3^- and at 30 μg/mL Tc, the uptake of Tc after 20 minutes was approximately 8.2 mg/g of adsorbent, which suggests that the NO_3^- ions are about 80 times less effective than Tc in competing for the sites on the adsorbent where TcO_4^- can be reduced. This confirms the suggestions made by Moyer and Bonnesen (42) who highlighted the factors that increase the affinity of an anion for a site, such as a large size, a small charge-to-size ratio, and a low hydration energy. For ions with a single negative charge, the hydration energy systematically decreases as the size of the anion increases. Divalent anions, such as sulfate, have a relatively high charge density and consequently have a relatively high hydration energy. The pertechnetate ion has a larger thermochemical radius than does NO_3, 0.255 nm compared with 0.196 nm, and a lower hydration energy, −244 kJ/mol compared with −314 kJ/mol. These experiments showed that an intrinsic bias exists toward pertechnetate over NO_3^- in competition for the adsorption sites.

The surface area of the wet adsorbent has been estimated at 500 m^2/g (21), so that in sample 1 with a Tc uptake of 0.9 mg/g, the average area occupied by each Tc atoms was approximately 10 nm × 10 nm. For sample 2, in which the uptake was 8.2 mg/g, the area occupied by each Tc atoms is 3 nm × 3 nm. However, the best fit to the EXAFS data results suggests that in both cases the distance between neighboring Tc atoms is 0.32 nm. This suggests that the pertechnetate uptake sites are in adjacent pairs.

Historically, removal of TcO_4^- has been achieved by the use of strongly basic anion-exchange resins. However, the very high concentration of competing nitrate ion makes this operation relatively inefficient, thus generating a large volume of contaminated spent resin for storage or disposal. Also, the presence of adsorbed nitrate on an amine-type resin is thermodynamically unstable and may present a potential hazard when spent resin is stored.

Bostick et al. (32–34) are concerned with the control of technetium in industrial processing of nuclear materials, such as heavy-metal sludge filtrate. Various uranium recovery, machine cleaning, and decontamination activities at gaseous diffusion plants produce an aqueous mixed-waste stream (raffinate) containing high concentrations of nitric acid and toxic heavy metals together with trace levels of radioactive U and Tc. This waste is diluted and the solution pH adjusted to a slightly alkaline value (approximately pH 8.0–8.5) to precipitate hydrolyzable metals and remove them by sludge filtration. This procedure is very effective for re-

moving iron, aluminum, and most toxic heavy metals (including uranium), but the filtrate contains some residual soluble species of regulatory concern, including mercury, technetium, and nitrate ions. Nitrate ions in the filtrate can be greatly reduced by biodenitrification, but toxic metals and radionuclides must first be removed to avoid forming voluminous amounts of contaminated biosludge that, as a low-level mixed waste, would not qualify for economical disposal in landfills.

Bostick et al. (32–34,43) have found that cross-linked polyvinylpyridine (PVP) resin is more efficient than strongly basic anion-exchange resin for removal of technetium in wastes containing high concentrations of nitrate ion, as shown in Table 10a. Resin loading by nitrate is greatly reduced by PVP, and PVP resins are very stable with respect to chemical and radiological degradation. After 24 hours of equilibration of the heavy metal sludge filtrate, containing 13.7 mg/L of Tc and 142 g/L (2.3 mol/L) of nitrate with 25 g/L of various resins, it was found that PVP was most effective at reducing Tc concentration. However, the uptake and the speed of uptake were poor compared with the biologically produced (Table 7b) material. However, the chemically precipitated greigite reduced Tc to 11.4 mg/L, an uptake of 0.084 mg/g or approximately 10 times less than the uptake shown by biologically produced adsorbents (Table 7b). The addition of 50 g of greigite per liter reduced Tc to 0.04 mg/L corresponding to an uptake of 0.27 mg/g. Bostick et al. also found that an addition of zero-valent iron produced similar results to those experiments in which the chemically precipitated greigite was used. Bostick et al. concluded that zero-valent iron and greigite were the most effective materials to treat the heavy-metal sludge filtrate but also suggested that if the surface area of the materials could be increased, the equilibration times could be reduced. The chemically produced greigite has a maximum surface area of 10 m^2/g, whereas the value for the microbiologically produced adsorbent material is approximately 500 m^2/g, which is a contributing factor to the short equilibration times of the biologically generated adsorbent (Table 7b). Furthermore, if the adsorption of a radionuclide is undertaken so that the adsorbent acts as a carrier material for long-term storage of the radionuclide, the quantity of uptake should be as high as possible. The uptake by the zero-valent iron and the greigite described by Bostick et al. (32–34) are less than the biologically generated iron sulfides, but more work needs to be done to clarify these differences along with the effects of pH and interfering ions, such as bicarbonate and nitrate. However the speed and relatively high uptake created by the biologically generated material are clear advantages for its use.

After studying a series of pertechnetate ion measurements to those of a series of commercially available resins, Brown et al. (44–45) concluded that pertechnetate was adsorbed much more strongly to resins with a polystyrene backbone than to resins with an acrylic or PVP backbone, such as those that had been studied by Bostick et al. (32–34,43) as shown in Table 10b. Brown et al. (44) discussed the development of resins with enhanced selectivity for the pertechnetate anion over other anions commonly found in groundwater, such bicarbonate, chloride, sulfate, or nitrate.

MARCEL DEKKER, INC.
270 Madison Avenue, New York, New York 10016

Table 10a. TcO_4^- Removal from High-Nitrate Heavy-Metal Sludge Filtrate

	Tc = 0.2 mg/L and NO_3^- = 210 g/L			Tc = 13.7 mg/L and NO_3^- = 142 g/L		
Adsorbent	Wt/L g/L	*Kc* (mL/g)	Uptake (mg/g)	Wt/L (mL/g)	*Kc* (mL/g)	Uptake (mg/g)
Iron metal	10	3.3233×10^4	0.020	50	2720	0.28
Fe_3S4	10	1.166×10^3	0.019	100	1360	0.14
				50	7968	0.27
				25	626	0.52
				10	733	1.21
Reillex 402	10	312	0.015	100	1240	0.136
Dowex SRB-OH	10	88	9.36×10^{-3}	90	267	0.146
Amberlite A-26	10	60	7.46×19^{-3}			
Reillex 202	10	47	6.36×10^{-3}			

Data from (31).
The Samples were allowed to equilibrate for 24 hours before measurements were taken.

The coefficient of sorption, *Kc*, of the bacterially generated adsorbent had similar values to the that of ion-exchange resins made at Oak Ridge National Laboratory (ORNL) specifically for the pertechnetate ion. However, the time required to reach equilibrium was at least 1 order of magnitude faster for the bacterially generated adsorbents than for the ORNL resins (44–46).

Table 10b. TcO_4^- Removal from Low-Nitrate Groundwater Test Solution

Adsorbent	Kc (mL/g)	Equilibration Time (h)	Type
VP02-165	4.17×10^4	24	Vinylbenzyl Cl cross-linked with divinylbenzene
VP02-122	3.45×10^4	24	
Reillex HPQ	4.54×10^3	24	Polyvinylpyridine
Purolite® A-850	1.02×10^2	24	Polystyrene
Amberlite IRA-900	2.46×10^3	24	Polystyrene
Amberlite IRA-904	7.59×10^3	24	Polystyrene
Purolite® A-520E	11.3×10^4	24	Polystyrene
Sybron Ionac® SR-7	6.95×10^3	24	Polystyrene
Sybron Ionac® SR-6	20.7×10^4	24	Polystyrene

Data from (52, 53).
VPO2-165 and VPO2-122 are not commercially available. Tc = 0.590 mg/L; NO_3^- = 3.72 g/L.

MARCEL DEKKER, INC.
270 Madison Avenue, New York, New York 10016

Resins with superior pertechnetate selectivity and breakthrough performance in column flow-through experiments could be obtained by incorporating 2 different types of strongly basic anion-exchange sites into the resin and are important innovations (46,47). These novel bifunctional resins are designed to incorporate resin-exchange sites that are highly selective for pertechnetate but kinetically slow with sites that are less selective but kinetically fast. The resulting bifunctional resins have superior selectivity and the same or better exchange capacity than resins prepared from single trialkyl amines, such as tripropyl or tributylamine, but that possess equivalent or faster exchange kinetics.

Brown and Gu (48) completed a field demonstration of the bifunctional anion-exchange resin (BiQuat) at the Northwest Plume Treatment facility at the Paducah Gaseous Diffusion Plant, Kentucky, at the end of 1999. In this test, a column 13.34 cm in diameter by 30.48 cm in length treated approximately 3.18×10^6 L of Tc-contaminated groundwater at a level of 99 ng/L. The system had a nominal flow rate of 568 L/h, and breakthrough was not observed in the column effluent. Sampling ports at the first 1/3 of the column and second 2/3 of the column indicated complete breakthrough at the first port and 20% breakthrough at the second port. This amounts to an uptake of 0.2 g/L or 0.023 mg/g by the resin, which is only 0.15% of the total ion exchange capacity of the resin because the column residence time of the fluid was 27 seconds. The uptake kinetics are the limiting conditions of performances. The composition of the stripping solution for the Tc is proprietary, but the performance should be such that 20 bed volumes of solution will remove the pertechnetate from a single bed volume of resin. If 0.34 m^3 of resin treats a 0.378 m^3 per minute stream and adsorption occurs on the resin for 1 year and is followed by stripping the bed with 20 bed volumes, a Tc-volume concentration of approximately 2.8 mg/L will result. Based on the data presented in Table 7b, sample 2, adding 0.27 mg/L, 1.8 kg in total, of the biologically generated iron sulfide would reduce the concentration within the 6.8 m^3 from 2.5 mg/L to 0.3 mg/L within 20 minutes.

CONCLUSIONS

Microbiologically produced, strongly magnetic iron sulfide is a good adsorbent for a wide variety of metal ions, including many connected with the nuclear industry, which makes the pertechnetate ion of special interest. The adsorbent is effective over a wide range of ion concentrations from 30 g/L to ng/L levels and below. However, the data presented in Tables 1, 2, 7a, and 7b show that a number of unexplained results require further work.

Although other ion exchange resins have been produced for the adsorption of these materials; the bacterially generated material appears to have a number

MARCEL DEKKER, INC.
270 Madison Avenue, New York, New York 10016

of important advantages. First, the uptake of heavy metals is very rapid and in the case of the more specific resin for Tc, the uptake kinetics are slow and the time taken for equilibrium to be reached is greater by at least 1 order of magnitude.

Second, the biologically generated adsorbent can be manufactured in the same form on a large-scale (49) for many applications, such as the recovery of heavy metals for the nuclear industry, the recovery of metals for the precious metals industry, pollution control for both heavy metals and the chloro- and fluorocarbon compounds, and in recycling materials from electronics and other industries (50). The cost of the normal ion-exchange resin is between $8–12 per liter and that for the biologically generated material is estimated to be $8–15 per liter. The slight difference in price is perhaps off-set by the speed of uptake and the capacity of the material for adsorbed heavy metals (2). The biologically generated material should be cheaper than an adsorbent, such as the $60/L BiQuat resin, that is especially tailored for Tc with very specific application areas (G. M. Brown, Oak Ridge National Laboratory, Private Communication, February 2000).

Third, the highly magnetic nature of the iron sulfide material makes recovery cheap and rapid with simple magnetic separators. Using HGMS (15–18) with an applied field of 1 T, the adsorbent can be extracted from solution at a fluid velocity of 8×10^{-2} m/s. A commercially available separator channel (18) of 1 m^2 and a separator duty factor of 0.75, will process the suspension at a rate of 220 m^3/h and at a cost, including the depreciation of the machine over a 10-year period, of $\$0.10/m^3$.

The limitations of the biologically generated iron sulfide adsorbent are important considerations for its use. First, the adsorbent is soluble in acid solutions so that its application range corresponds to pH >5.5.

Second, the material oxidizes in air or in suspensions exposed to air, and therefore, it must be stored anaerobically. When stored anaerobically, it retains the adsorbent and magnetic properties discussed in reference to Table 7b. When the material is freeze-dried it is much more stable in air and in suspensions exposed to air due probably to the reduction in surface area.

Many areas of application exist for this adsorbent material, and much more work needs to be done to elucidate the adsorption process. The nuclear industry may represent one potential application area. However, questions need to be investigated.

For the purposes of long-term storage in the nuclear industry, is this material suitable for encapsulation, and would it require extensive treatment for safe long-term storage? Freeze-drying reduces the surface area from at least 500 m^2/g to 18.4 m^2/g. However, neutron scattering shows 2-nm holes remain within the freeze-dried material (21). Consequently, if the iron sulfide is freeze-dried after

MARCEL DEKKER, INC.
270 Madison Avenue, New York, New York 10016

the adsorption of the radioactive substances has taken place, are radionuclides incorporated on the surface of these internal pores? These pores are inaccessible to the N_2 gas used to measure the surface area (29), which suggests that the pores are significantly isolated from the outside environment. The potential usefulness of this process needs to be explored.

Also, SRB can be widely found in anaerobic sedimentary environments, such as rivers, estuaries, harbors, salt marshes, lakes, canals, and the deep sea. These bacteria, in the past on a geological timescale, were responsible for many large iron-sulfide deposits. In this work, the main interest is the occurrence of SRB in sediments and the implications of their potential for heavy metal immobilization (51). If heavy metals, with insoluble sulfides, are present in a suitably liberated form, they will be precipitated at pH 7 onto the surface of the bacterium (52–56). As the buildup of the metal sulfide proceeds, much of the material can become detached from the bacterium surface and form mineral particles within the sediment. In 2000, Rozan et al. (57) found evidence for iron, copper, and zinc complexation as multinuclear sulfide clusters in 4 toxic rivers in Connecticut and Maryland; this may be evidence for the action of SRB. Many surveys of the heavy metal content of sediments have been conducted in rivers, salt marshes, bays, lagoons, and harbors throughout the world, and many of the heavy metal deposits are associated with sulfur and have been attributed to the action of SRB (28,52,54,58–70). If sediments are left undisturbed, these immobilization processes are extremely beneficial because they prevent the heavy metals from entering the food chain. Can these naturally occurring processes be engineered to contain and prevent the spread of heavy metal release into the environment?

ACKNOWLEDGMENTS

The authors wish to acknowledge the provision of time on DARTS, the UK national synchrotron radiation service at the CLRC Daresbury Laboratory, and ISIS, the pulsed neutron facility at the Rutherford-Appleton Laboratory. We are grateful to Prof D. J. Vaughan and Dr. R. A. D. Pattrick of the Department of Earth Sciences, Manchester University, for making available the XANES spectra of the iron sulfide model compounds; to Dr Bill Bostick, MCL Inc; and to Dr Gilbert Brown, ORNL, for much appreciated private communication. We also wish to thank colleagues at the University of Southampton, namely, Profs Brian Rainford, Peter de Groot and George Attard, and Drs. Alan Howard, and Andrew P. Roberts, for useful discussion. We also gratefully acknowledge financial support from Biopraxis Developments Ltd, the Office of Innovation and Research Support at the University of Southampton, Southampton Innovation Ltd, and NSG Environmental Ltd.

REFERENCES

1. Watson, J.H.P.; Ellwood, D.C.; Duggleby, C.J. A Chemostat with Magnetic Feedback for the Growth of Sulfate Reducing Bacteria and Its Application to the Removal and Recovery of Heavy Metals from Solution. Minerals Eng. **1996,** *9*, 973–983.
2. Watson, J.H.P.; Ellwood, D.C.; Deng, Q.; Mikhalovsky, S.; Hayter, C.E.; Evans, J. Heavy Metal Adsorption on Bacterially Produced FeS. Minerals Eng. **1995,** *8*,1097–1108.
3. Trebalka, J.R.; Garten, C.T., Jr. Behaviour of the Long-Lived Synthetic Elements and Their Natural Analogues in Food Chains. In *Advances in Radiobiology*; Lett, J.T., Ehman, U.K., Cox, A.B., Eds.; Academic Press Ltd: London, 1983; Vol. 10, 68–73.
4. Macaskie, L.E. The Application of Biotechnology to the Treatment of Wastes Produced from the Nuclear Fuel Cycle: Biodegradation and Bioaccumulation as a Means of Treating Radionuclide-Containing Streams. Crit. Revs. Biotechnol. **1991,** *11*, 41–112.
5. Wildung, R.E.; McFadden, K.M.; Garland, T.R. Technetium Sources and Behavior in the Environment. J. Environ. Qual., **1979,** *8,* 156–161.
6. Cataldo, D.A.; Garland, T.R.; Wildung, R.E.; Fellows, R.J. Comparative Metabolic Behaviour and Interrelationships of Tc and S in Soybean Plants. Health Phys. **1989,** *57,* 281–288.
7. Camplin, W.C. *Radioactivity in Food and the Environment, 1995,* Ministry of Agriculture, Fisheries and Food RIFE-1, 1996.
8. Environmental Data Services. *Radioactive Lobsters Put Squeeze on Sellafield*, Environmental Data Services No. 262; Author: London, Nov. 1996.
9. Bolton, L., *BNFL pressed on radioactivity,* Financial Times, p 6, December 14, 1996.
10. Schroeder, N.C.; Radzinski, S.; Ashley, K.R.; Ball, J.; Stamore, F.; Whitener, G. *Technetium Partitioning for the Hanford Tank Waste Remediation: Sorption of Technetium from DSS and DSSF7 Waste Simulants Using Reillex™ - HPQ Resin*, Los Alamos National Laboratory LALP 95-174; Los Alamos, NM, 1996.
11. Watson, J.H.P.; Ellwood, D.C. Biomagnetic Separation and Extraction Process. IEEE Trans. Magn., **1987,** *MAG-23,* 3751–3752.
12. Watson, J.H.P.; Ellwood, D.C. A Biomagnetic Separation Process for the Removal of Heavy Metal Ions from Solution, presented at the International Conference on Control of Environmental Problems from Metal Mines, Roros, Norway, June 20–24, 1988.
13. Ellwood, D.C., Hill, M.J. and Watson, J.H.P., "Pollution Control using Microorganisms and Magnetic Separation," in *Microbial Control of Pollution, Symposia of the Society of General Microbiology,* Fry, J.C., Eds., Gadd,

MARCEL DEKKER, INC.
270 Madison Avenue, New York, New York 10016

G.M., Herbert, R.A., Jones, C.W., and Watson-Craik, I.A. Cambridge, UK: Cambridge University Press, **1992,** pp. 89–112.
14. Watson, J.H.P.; Ellwood, D.C. Biomagnetic Separation and Extraction Process for Heavy Metals from Solution. Minerals Eng. **1994,** *7*, 1017–1028.
15. Watson, J.H.P. Magnetic Filtration. J. Appl. Phys. **1973,** *44,* 4209–4213.
16. Svoboda, J. Magnetic Methods for the Treatment of Minerals, 1st Ed.; In *Developments in Mineral Processing,* Fuerstenau, D.W., Ed.; Elsevier: Amsterdam, 1987; Vol. 8.
17. Marston, P.G.; Nolan, J.J.; Lontai, L.M. Magnetic Separator and Magnetic/Separation Method. US Patent 3,627,678, December 14, 1971.
18. Watson, J.H.P. Superconducting Magnetic Separation. In *Handbook of Applied Superconductivity*, 1st Ed.; Seeber, B., Ed.; Institute of Physics Publishing: Bristol, UK, 1998; Vol. 2, 1371–1406.
19. Keller-Besrest, F.; Collin, G. II Structural Aspects of the α Transition in Off-Stoichiometric $Fe_{1-x}S$ Crystals. J. Sol. State Chem. **1990,** *84,* 211–225.
20. Waychunas, G.A.; Apted, M.J.; Brown, G.E., Jr. X-ray K-Edge Absorption Spectra of Fe Minerals and Model Compounds: Near-Edge Structure. Phys. Chem. Min. **1983,** *10,* 1–9.
21. Watson, J.H.P.; Cressey, B.A.; Roberts, A.P.; Ellwood, D.C.; Charnock, J.M.; Soper, A.K. Structural and Magnetic Studies on Heavy-Metal-Adsorbing Iron Sulfide Nanoparticles Produced by Sulfate-Reducing Bacteria. J. Mag. Mag. Mat. **2000,** *214*, 13–30.
22. Watson, J.H.P.; Ellwood, D.C.; Soper, A.K.; Charnock, J. Nanosized Strongly-Magnetic Bacterially-Produced Iron Sulfide. J. Mag. Mag. Mat. **1999,** *203,* 69–72.
23. Schwarz, E.J.; Vaughan, D.J. Magnetic Phase Relations of Pyrrhotite. J. Geomag. Geoelectr. **1972,** *24,* 441–458.
24. Power, L.F.; Fine, H.A. The Iron-Sulphur System, Part 1, The Structures and Physical Properties of the Compounds of the Low-Temperature Phase Fields. Minerals Sci. Engng. **1976,** *8,* 106–128.
25. Skinner, B.J.; Erd, R.C.; Grimaldi, F.S. Greigite, the Thio-Spinel of Iron: a New Mineral. Am. Mineralogist, **1964,** *49,* 543–555.
26. Spender, M.R.; Coey, J.M.D.; Morrish, A.H. The Magnetic Properties and Mossbauer Spectra of Synthetic Samples of Fe_3S_4. Can. J. Phys. **1972,** *50,* 2313–2326.
27. Watson, J.H.P.; Ellwood, D.C. Feedback Chemostat. British Patent Application GB 9516753.2., 1995.
28. Roberts, A.P. Magnetic Properties of Sedimentary Greigite (Fe_3S_4). Earth Planet. Sci. Lett. **1995,** *134,* 227–236.
29. Brunauer, S.; Emmett, P.H.; Teller, E. The Adsorption of Gases and Vapours. J. Am. Chem. Soc. **1938,** *60,* 309.
30. Stockdale, J.A.D.; Bostick, W.D.; Hoffmann, D.P.; Lee, H.T. *Surrogate Formulations for Thermal Treatment of Low-Level Mixed Waste: Part 1:*

MARCEL DEKKER, INC.
270 Madison Avenue, New York, New York 10016

Radiological Surrogates, DOE/MWIP-15; Martin Marietta Energy Systems, Inc: Oak Ridge, Tenn, 1994.
31. McCarthy, J.F.; Sanford, W.E.; Stafford, P.L. Lanthanide Field Tracers Demonstrate Enhanced Transport of Transuranic Radionuclides by Organic Matter. Environ. Sci. Technol. **1998,** *32,* 3901–3906.
32. Bostick, W.D.; Evans-Brown, B.S. *Sorptive Removal of Technetium from Heavy Metal Sludge Filtrate Containing Nitrate Ion*, USA K/QT-160-P, DE 88 010156; Oak Ridge Gaseous Diffusion Plant operated by Martin Marietta Energy Systems, Inc: Oak Ridge, Tenn, 1988.
33. Bostick, W.D.; Shoemaker, J.L.; Osborne, P.E.; Evans-Brown, B. Treatment and Disposal Options for a Heavy Metals Waste Containing Soluble Technetium-99. In *Emerging Technologies in Hazardous Waste Management*; American Chemical Society Symposium Series 422; Tedder, D.W., Pohland, F.G., Eds.; American Chemical Society: Washington, DC, 1990; 345–367.
34. Del Cul, G.D., Bostick, W.D., Trotter, D.R. and Osborne, P.E. "Technetium-99 removal from process solutions and contaminated groundwater," **1993,** *Separation Science and Technology,* vol. **28,** pp. 551–564.
35. Binstead, N.; Campbell, J.W.; Gurman, S.J.; Stephenson, P.C. EXCURV 92; Daresbury Laboratory, Daresbury, Warrington, England, 1991.
36. Lee, P.A.; Pendry, J.B. Theory of the Extended X-ray Absorption Fine Structure. Phys. Rev. **1975,** *B11,* 2795–2811.
37. Gurman, S.J.; Binstead, N.; Ross, I. A Rapid, Exact, Curved Wave Theory for EXAFS Calculations. J. Phys. C. **1984,** *17,* 143–151.
38. Hedin, L.; Lundqvist, S. Effects of Electron-Electron and Electron-Phonon Interactions on the One-Electron States of Solids. Sol. State Phys., **1969,** *23,*1–181.
39. Faggiani, R.; Lock, C.J.L.; Poce, J. The Structure of Ammonium Pertechnetate At 295, 208 and 141 K. Acta Crystall. B **1980,** *36,* 231–233.
40. Almahamid, I; Bryan, J.C.; Bucher, J.J.; Burrell, A.K.; Edelstein, N.M.; Hudson, E.A.; Kaltsoyannis, N.; Lukens, W.W.; Shuh, D.K.; Nitsche, H.; Reich, T. Electronic and Structural Investigations of Technetium Compounds by X-ray Absorption Spectroscopy. Inorg. Chem. **1995,** *34,* 193–198.
41. Haines, R.I.; Owen, D.G.; Vandergraaf, T.T. Technetium–Iron Oxide Reactions Under Anaerobic Conditions: A Fourier Transform Infrared, FTIR Study. Nuclear Journal of Canada **1987,** *1,* 32–37.
42. Moyer, B.A.; Bonnesen, P.V. Physical Factors in Anion Separations. In *Supramolecular Chemistry of Anions*; Bianchi, A., Bowman-James, K., Garcia-Espana, E., Eds.; John Wiley, Inc: New York, 1997.
43. Del Cul, G.D.; Bostick, W.D.; Trotter, D.R.; Osborne, P.E. Technetium-99 Removal from Process Solutions and Contaminated Groundwater. Sep. Sci. Tech. **1993,** *28,* 551–564.
44. Brown, G.M.; Bonneson, P.V.; Moyer, B.A.; Gu, B.; Alexandratos, S.D.; Patel, V.; Oder, R. The Design of Resins for the Removal of Pertechnetate

MARCEL DEKKER, INC.
270 Madison Avenue, New York, New York 10016

and Perchlorate from Groundwater. In *Perchlorate in the Environment*; Urbansky, E.T., Ed.; American Chemical Society: Washington, DC, 2000.
45. Bonnesen, P.V.; Alexandratov, S.D.; Brown, G.M.; Hussain, L.A.; Moyer, B.A.; Patel, V. Selective Resins for Sorption of Technetium from Groundwater, presented at the American Institute of Chemical Engineers 1995 Annual Meeting, Miami, Fla, Nov 12–17, 1995.
46. Alexandratos, S.D.; Brown, G.M.; Bonneson, P.V.; Moyer, B.A. Bifunctional Anion-Exchange Resins with Improved Selectivity and Exchange Kinetics. US Patent 6,059,975, May 9, 2000.
47. Bonnesen, P.V.; Brown, G.M.; Alexandratos, S.D.; Bavoux, L.B.; Presley, D.J.; Patel, V.; Moyer, B.A. Development of Bifunctional Anion Exchange Resins with Improved Selectivity and Sorptive Kinetics for Pertechnetate. Batch-Equilibrium Experiments. Environ. Sci. Technol. **2000,** *34,* 3761–3766.
48. Gu, B., Brown, G.M., Bonnesen, P.V., Liang, L., Moyer, B.A., Ober, R., Alexandratos, S.D. **2000.** Development of Novel Bifunctional Anion-Exchange Resins with Improved Selectivity for Pertechnetate: Column Breakthrough and Field Studies. Environ. Sci. Technol. 34:1075–1080.
49. Barnes, L.J.; Janssen, F.J.; Scheeren, P.J.H.; Versteegh, J.H.; Koch, R.O. Simultaneous Microbial Removal of Sulphate and Heavy Metal Ions from Waste Water. Trans. Instn. Min. Metall., Section C **1992,** *101,* C183–C189.
50. Watson, J.H.P.; Ellwood, D.C. The Removal of Heavy Metals from Solution Using Bacterially-Produced Adsorbents, presented at Environmental Strategies for the 21st Century—An Asia Pacific Conference, Pan Pacific Hotel, Singapore, April 8–10, 1998.
51. Odam, J.M. Industrial and Environmental Activities of Sulfate-Reducing Bacteria. In *The Sulfate-Reducing Bacteria: Contemporary Perspectives*; Brock/Springer Series in Contemporary Bioscience; Odam, J.M., Singleton, R., Jr., Eds.; Springer-Verlag: New York, 1993; 189–210.
52. Jørgensen, B.B. Bacterial Sulfate Reduction Within Reduced Microniches of Oxidized Marine Sediments. Mar. Biol. **1977,** *41,* 7–17.
53. Henrot, J. Bioaccumulation and Chemical Modification of Technetium by Soil Bacteria. Health Phys. **1989,** *57,* 239–245.
54. Revis, N.W.; Elmore, J.; Edenborn, H.; Osborne, T.; Holdsworth, G.; Hodden, C.; King, A. Immobilization of Mercury and Other Heavy Metals in Soil, Sediment, Sludge and Water by Sulfate-Reducing Bacteria. In *Biological Processes*; Innovative Hazardous Waste Treatment Series; W.H. Freeman and Co.: San Francisco, CA, 1991; Vol. 3, 97–105.
55. Watson, J.H.P.; Ellwood, D.C.; Hamilton, E.O.; Mills, J. The Removal of Heavy Metals and Organic Compounds from Anaerobic Sludges, presented at the Congress on Characterisation and Treatment of Sludge, Gent, Belgium, Feb 26–March 1 1991.
56. Lloyd, J.R.; Thomas, G.H.; Finlay, J.A.; Cole, J.A.; Macaskie, L.E. Microbial Reduction of Technetium by *Escherichia coli* and *Desulfovibrio desul-*

MARCEL DEKKER, INC.
270 Madison Avenue, New York, New York 10016

furicans: Enhancement Via the Use of High-Activity Strains and Effect of Process Parameters. Biotechnol. Bioeng. **1999,** *66,* 122–130.
57. Rozan, T.F.; Lassman, M.E.; Ridge, D.P.; Luther III, G.W. Evidence for Iron, Copper and Zinc Complexation as Multinuclear Sulphide Clusters in Oxic Revers. Nature **2000,** *406,* 879–882.
58. Hilton, J.; Lishman, J.P.; Chapman, J.S. Magnetic and Chemical Characterisation of a Diagenetic Magnetic Mineral Formed in the Sediments of Productive Lakes. Chem. Geol. **1986,** *56,* 325–333.
59. Hilton, J.; Long, G.J.; Chapman, J.S.; Lishman, J.P. Iron Mineralogy in Sediments: A Mossbauer Study. Geochim. Cosmochim. Acta **1986,** *50,* 2147–2151.
60. Hilton, J. A Simple Model for the Interpretation of Magnetic Records in Lacustrine and Ocean Sediments. Quat. Res. **1987,** *27,* 160–166.
61. Hilton, J. Greigite and the Magnetic Properties of Sediments. Limnol. Oceanogr. **1990,** *35,* 509–520.
62. Arakaki, T.; Morse, J.W. Coprecipitation and Adsorption of Mn(II) with Mackinawite (FeS) Under Conditions Found in Anoxic Sediments. Geochim. Cosmochim. Acta **1993,** *57,* 9–14.
63. Panchanadikar, V.V.; Kar, R.N. Precipitation of Copper Using *Desulfovibrio sp.* World J. Microbiol. Biotechnol. **1993,** *8,* 280–281.
64. Tebo, B.M. Metal Precipitation by Marine Bacteria: Potential for Biotechnological Applications. In *Genetic Engineering*; Setlow, J.K., Ed.; Plenum Press: New York, 1995; 231–263.
65. Verosub, K.L.; Roberts, A.P. Environmental Magnetism: Past, Present And Future. J. Geophys. Res. **1995,** *100,* 2175–2192.
66. Roberts, A.P.; Turner, G.M. Diagenetic Formation of Ferrimagnetic Iron Sulphide Minerals in Rapidly Deposited Marine Sediments, South Island, New Zealand. Earth Plan. Sci. Lett. **1993,** *115,* 257–273.
67. Roberts, A.P.; Reynolds, R.L.; Verosub, K.L.; Adam, D.P. Environmental Magnetic Implications of Greigite (Fe_3S_4) Formation in a 3 M.Y. Lake Sediment Record from Butte Valley, Northern California. Geophysic. Res. Lett. **1996,** *23,* 2859–2862.
68. Cooper, D.C.; Morse, J.W. Biogeochemical Controls on Trace Metal Cycling in Anoxic Marine Sediments. Environ. Sci. Technol. **1998,** *32,* 327–330.
69. Cooper, D.C.; Morse, J.W. Extractability of Metal Sulfide Minerals in Acidic Solutions: Application to Environmental Studies of Trace Metal Contamination within Anoxic Sediments. Environ. Sci. Technol. **1998,** *32,* 1076–1078.
70. Cooper, D.C.; Morse, J.W. Selective Extraction Chemistry of Toxic Metal Sulfides from Sediments. Aquat. Geochem. **1999,** *5,* 87–97.

Received July 2000
Revised November 2000

MARCEL DEKKER, INC.
270 Madison Avenue, New York, New York 10016

Request Permission or Order Reprints Instantly!